ELSEVIER

Journal of Photochemistry and Photobiology A: Chemistry 134 (2000) 155–161

Journal of Photochemistry and Photobiology A:Chemistry

www.elsevier.nl/locate/jphotochem

Photoreduction of methylviologen using methylacridine orange in the presence of triethanolamine in ethanol–water mixtures

Shafiqul D.-M. Islam, Yuko Yoshikawa [a], Mamoru Fujitsuka [a], Osamu Ito [a,*], Suguru Komatsu [b], Yoshiharu Usui [b]

[a] *Institute for Chemical Reaction Science, Tohoku University, Katahira, Aoba-ku, Sendai 980-8577, Japan*

[b] *Department of Environmental Science, Ibaraki University, Mito, Ibaraki, Japan*

Received 29 November 1999; received in revised form 24 February 2000; accepted 8 March 2000

Abstract

Photoreduction of methylviologen (MV^{2+}) by 10-methylacridine orange (MAO^{+}) in the presence of triethanolamine (TEOA) has been investigated in ethanol–water mixed solvents by means of steady-state and laser-flash photolysis in visible/near-IR regions. The complete conversion from MV^{2+} to $MV^{\bullet+}$ was observed under the condition of $[MV^{2+}]>[MAO^{+}]$ in the presence of an excess TEOA. By laser-flash photolysis measurements, the various rate constants for the electron transfer processes (k_{et}) have been determined. The k_{et} values for electron transfer from the triplet state of MAO^{+} ($^3(MAO^{+})^*$) to MV^{2+}, which is the initial step of oxidative route, are in the order of $10^8\ M^{-1}\ s^{-1}$. The rate constant of back electron transfer between the ion radicals ($MV^{\bullet+}$ and $(MAO^{+})^{\bullet+}$) was ca. $3\times10^8\ M^{-1}\ s^{-1}$, while the back electron-transfer process was suppressed on addition of TEOA. The k_{et} values from TEOA to $^3(MAO^{+})^*$, which is the initial step of reductive route, are in the order of $10^5\ M^{-1}\ s^{-1}$. The k_{et} value for electron transfer from $(MAO^{+})^{\bullet-}$ to MV^{2+} was estimated to be $4.7\times10^8\ M^{-1}\ s^{-1}$. Contributions of the oxidative and reductive routes of $^3(MAO^{+})^*$ to the $MV^{\bullet+}$ formation vary with TEOA concentration. High quantum yields for the $MV^{\bullet+}$ formation were evaluated. The effects of the ion salt and solvents on the rate constants and quantum yields were found.

Keywords: Methylacridine orange; Methylviologen; Laser photolysis; Electron transfer; Photoreduction

1. Introduction

The importance of dyes as photosensitizers in oxidation and reduction reactions has been very well recognized [1–6]. The organic dyes including acridine orange (AO; 3,6-bis-dimethylaminoacridine) have been found to be applicable to photo-redox devices for utilization of solar energy as an efficient photo-sensitizer [7–11]. However, only a few reports for the detailed mechanistic and kinetic studies on photosensitization reactions of AO dyes appeared [11–14]. For the utilization of light energy and the application to the optical devices in technology, the mechanistic and kinetic investigations of highly efficient photosensitized reactions have been required. Although there are some studies in the literature on the redox reactions and photosensitization reactions of AO dyes using the flash photolysis and pulse radiolysis techniques [11,13–17], no attempt has been found for the observation of the transient absorption in the near-IR region, where some intense transient absorption bands due to the excited states of AO dyes are expected to appear. The reported analysis of the transient absorption bands in the visible region seems to be insufficient owing to overlap with various absorption bands due to the species such as the triplet state and the ion radicals derived from the photoredox reagents [11,13–17].

Numerous photochemical investigations have long been made on the reduction of the methylviologen dication (MV^{2+}) as a model system for the photogeneration of electric and chemical energy [18–22]. Various photoexcitable substances have been used as sensitizers for production of the long-lived methylviologen radical cation ($MV^{\bullet+}$) in the presence of sacrificial electron donors such as triethanolamine (TEOA) [6,23]. No reports are available in the literature concerning the photosensitized reduction of MV^{2+} using 10-methylacridine orange (MAO^{+}) as a sensitizer in the presence of TEOA.

In our present study for the photosensitization reaction of MAO^{+}, we employed the laser flash photolysis technique using suitable photodiodes detectors for the wide wavelength

* Corresponding author. Tel.: +81-22-217-5610; fax: +81-22-217-5610.
E-mail address: ito@icrs.tohoku.ac.jp (O. Ito)

1010-6030/00/$ – see front matter
PII: S1010-6030(00)00266-5

region and wide timescale measurements, which gave us quite reliable observations for detailed mechanistic studies. Solvent effects and salt effects on the photoreduction of MV^{2+} were also found in our present study.

2. Experimental

2.1. Materials

10-Methylacridine orange (MAO^+, I^-) was prepared from AO by treatment with methyl iodide [11,17]. Commercially available triethanolamine (TEOA; Nakarai) and 1,1-dimethyl-4,4-bipyridinium ion (methylviologen, $MV^{2+}(Cl^-)_2$; Tokyo Kasei) were used. $NaClO_4$ (Kanto) was used to control the ionic strength of the sample solutions.

2.2. Steady-state photolysis

The steady-state photolysis of MAO^+ in Ar-saturated solutions containing MV^{2+} and/or TEOA was performed with light longer wavelength than 400 nm from Xe–Hg lamp (150 W). The formation of $MV^{\bullet+}$ was followed by observing the UV–VIS spectra, which were measured with a JASCO/V-570 spectrophotometer.

2.3. Laser flash photolysis

MAO^+ in solution containing MV^{2+} and/or TEOA was excited by 490 nm light from OPO laser (Continuum Surelite OPO, 4 ns fwhm, 15 mJ per pulse) pumped with Nd:YAG laser (Continuum Surelite II-10). For measurements of the transient absorption spectra in the visible region, a Si-APD (Hamamatsu Photonics, S5343) was used as a detector for a continuous Xe-monitor lamp. For the measurements in the near-IR region, an InGaAs-PIN photodiode (Hamamatsu Photonics, G5125-10) [24,25] was employed as a detector.

3. Results and discussion

3.1. Steady-state measurements

3.1.1. Absorption spectra

The steady-state absorption spectra of MAO^+ (1.0×10^{-4} M) are shown in Fig. 1. In ethanol, the absorption peaks appear at 495 nm (ε_{max}=8600 $M^{-1}\,cm^{-1}$) and 270 nm, which are very similar to those of protonated AO (AOH^+) [17]. In ethanol–water (1:1, v/v) mixed solvent, the intensities of the absorption peaks decreased as compared with those in ethanol, keeping the absorption shape almost unchanged. When the water content exceeded more than 80%, the absorption intensity of the main peak further decreased and the relative intensity of the shoulder

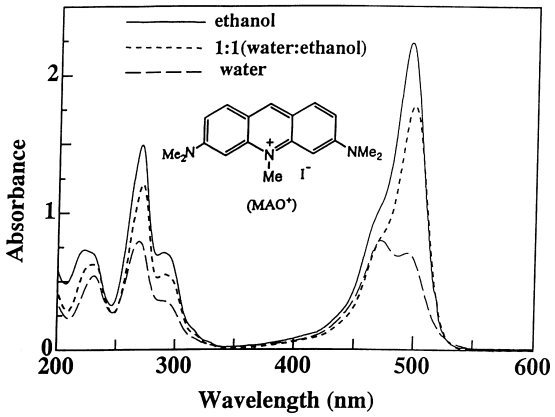

Fig. 1. Steady-state absorption spectra of MAO^+ (1.0×10^{-4} M) in ethanol, water–ethanol (1:1), and water; 2 mm optical path length.

at 460 nm increases. In water, the absorption intensity at 460 nm became higher than that at 495 nm, indicating the dimer formation of MAO^+ in water [26]. On addition of the quenchers (MV^{2+} and TEOA), no appreciable change due to the interaction of MAO^+ with MV^{2+} and TEOA was found at the ground state under the present experimental conditions.

3.1.2. Steady-state photolysis

By steady-light (>400 nm) illumination of MAO^+ in the presence of MV^{2+}, TEOA, and $NaClO_4$, the absorption bands appeared at 398 and 605 nm as shown in Fig. 2, which indicates the formation of $MV^{\bullet+}$ [13,27–29]. The absorption intensities of $MV^{\bullet+}$ increased with the illumination time, reaching a maximal concentration, which remained almost constant during the light illumination (inset of Fig. 2), indicating the stability of the photocycle system for the $MV^{\bullet+}$ generation. After switching off the light, the absorbance of $MV^{\bullet+}$ decreased slowly indicating that $MV^{\bullet+}$ is reoxidized

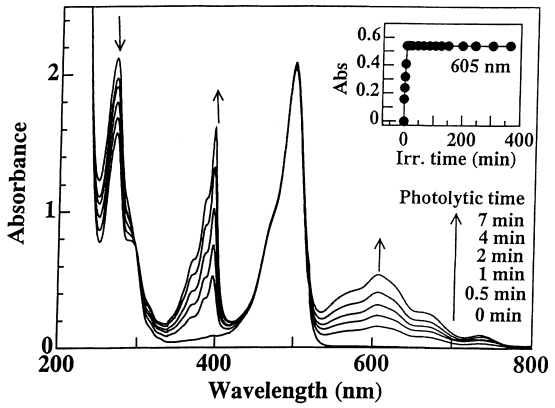

Fig. 2. Absorption spectral changes observed by steady photolysis of MAO^+ (1.0×10^{-4} M) with light (>400 nm) in the presence of MV^{2+} (2.0×10^{-4} M), TEOA (1.5×10^{-1} M), and $NaClO_4$ (2.0×10^{-2} M) in Ar-saturated ethanol–water (9:1, v/v) mixed solvent (2 mm optical path length). Inset: [$MV^{\bullet+}$] vs. irradiation time.

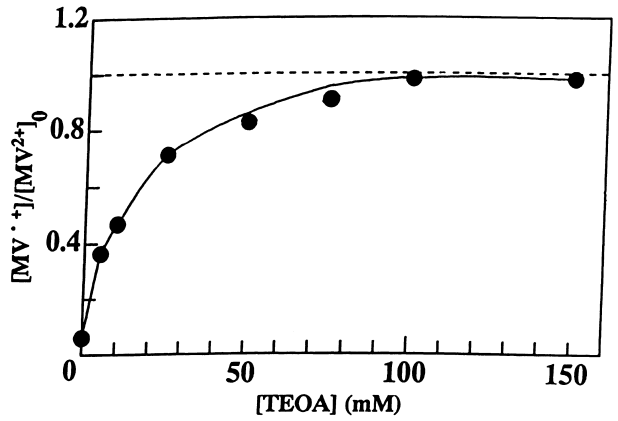

Fig. 3. Yields of $MV^{\bullet+}$ ($[MV^{\bullet+}]/[MV^{2+}]_0$) at various concentrations of TEOA. $[MAO^+]=1.0\times10^{-4}$ M, $[MV^{2+}]=2.0\times10^{-4}$ M, and $[NaClO_4]=2.0\times10^{-2}$ M in Ar-saturated ethanol–water (9:1, v/v) mixed solvent.

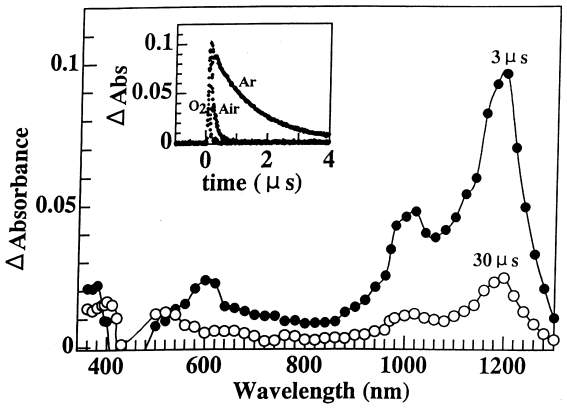

Fig. 4. Transient absorption spectra observed on photolysis of MAO^+ (1.0×10^{-4} M) with 490 nm-laser light in deaerated ethanol–water (4:1) mixed solvent; (●) 3 μs and (○) 30 μs. Inset: time profiles for quenching of $^3(MAO^+)^*$ with O_2 at 1200 nm.

to MV^{2+} in the dark. After the complete disappearance, $MV^{\bullet+}$ was regenerated by switching-on the light again, indicating that this system is reproducible. The main absorption peak of MAO^+ at 495 nm remained constant during the illumination (Fig. 2), which indicates the stability of effective MAO^+. The decrease in the absorbance at 265 nm is mainly due to the consumption of MV^{2+}.

3.1.3. Effect of TEOA concentration

The concentration of $MV^{\bullet+}$ was determined from the absorbance at 605 nm, taking $\varepsilon_{604\,nm}=1.37\times10^4\,M^{-1}\,cm^{-1}$ [28], from which the quantity $[MV^{\bullet+}]/[MV^{2+}]_0$ was calculated. This quantity increased with TEOA, saturating at high TEOA concentration (Fig. 3), which refers to Y_{SF} (steady-state $MV^{\bullet+}$ formation yield) [29]. The observed Y_{SF} values were found to decrease with an increase of water (Table 1), which may be due to the association of MAO^+ in water-rich mixed solvents. However, the lowest Y_{SF} values were found in 20 and 40% ethanol-containing mixed solvents. These findings may be due to specific interaction between ethanol and water, which may be related with the destruction of water-cluster by ethanol as reported in [30,31].

As an effect of TEOA, it is considered that TEOA donates an electron to the radical cation of MAO^+ ($(MAO^+)^{\bullet+}$), which is produced by donating electron to MV^{2+} via the photoexcited MAO^+; this process is denoted as oxidative route. Thus, the reproduced MAO^+ can be used again to reduce MV^{2+}, resulting in an increase of $MV^{\bullet+}$. As another cycle, it is also possible to consider that the photoexcited MAO^+ accepts an electron from TEOA producing the anion radical of MAO^+ ($(MAO^+)^{\bullet-}$), which donates an excess electron to MV^{2+} to form $MV^{\bullet+}$; this process is denoted as reductive route. In order to discriminate these two routes, it is necessary to perform the laser-flash photolysis study for this system.

3.2. Laser flash photolysis measurements

3.2.1. Triplet states

The transient absorption spectra obtained by the 490 nm-laser irradiation of MAO^+ are shown in Fig. 4. The absorption bands at 1200 and 1020 nm were attributed to

Table 1
Lifetimes of $^3(MAO^+)^*$ in absence (τ_T^0) and presence of ionic salt ($\tau_T^{0/I}$); rate constants for the quenching of $^3(MAO^+)^*$ in presence of (a) MV^{2+} (k_{et}^V); (b) MV^{2+}/ionic salt ($k_{et}^{V/I}$); (c) MV^{2+}/ionic salt/TEOA ($k_{et}^{V/I/A}$) in ethanol–water mixed solvents; Y_{SF} (=$[MV^{\bullet+}]/[MV^{2+}]_0$) and $\Phi_{MV^{\bullet+}}$ (=$[MV^{\bullet+}]/[^3(MAO^+)^*]$) at $[TEOA]=1.0\times10^{-1}$ M

EtOH (%)	τ_T^0 (μs)	$\tau_T^{0/I}$ (μs)	k_{et}^V ($M^{-1}\,s^{-1}$)	$k_{et}^{V/I}$ ($M^{-1}\,s^{-1}$)	$k_{et}^{V/I/A}$ ($M^{-1}\,s^{-1}$)	Y_{SF}	$\Phi_{MV^{\bullet+}}$
0	100	–[a]	5.8×10^8	–[a]	–[a]	0.65	0.64
20	59	15	3.9×10^8	–[a]	–[a]	0.38	0.34
40	220	59	1.8×10^8	5.6×10^8	1.3×10^9	0.60	0.58
60	180	67	1.5×10^8	5.0×10^8	7.3×10^8	0.76	0.64
80	26	43	1.8×10^8	7.6×10^8	1.3×10^9	0.82	0.70
90	10	20	3.0×10^8	6.7×10^8	1.2×10^9	0.95	0.82
100	1	–[b]	6.4×10^8	–[b]	–[b]	1.00	0.92

[a] In the presence of ionic salt, T–T absorption intensity decreased much so that the decay kinetics could not be followed.
[b] Low solubility of the salt.

the triplet state of MAO^+ ($^3(MAO^+)^*$) [32]. In the shorter wavelength regions, two bands at 400 and 600 nm also appeared, which are also attributed to $^3(MAO^+)^*$ [17]. Immediately after a laser pulse, a negative absorbance was observed in the 410–510 nm region, which is attributed to the depletion of the MAO^+ absorption. In the water-rich mixed solvents, the absorption of $^3(MAO^+)^*$ at 1200 nm was slightly broader than that in ethanol-rich solvents with keeping the peak position almost same, which is similar tendency to the ground state absorptions of MAO^+ (Fig. 1).

Under the dilute condition of MAO^+, the decay rates were not increased by the increase in the laser power, suggesting that T–T annihilation does not occur. On the other hand, the decay rates of $^3(MAO^+)^*$ increased with the ground state MAO^+ concentration, suggesting that $^3(MAO^+)^*$ reacts with ground state MAO^+ (self-quenching process). The self-quenching rate constant (k_{sq}) was evaluated from Eq. (1) [33].

$$\frac{1}{\tau_T} = \frac{1}{\tau_T^0} + k_{sq}[MAO^+] \quad (1)$$

where the τ_T refers to the lifetime calculated from the observed first-order rate constant ($k_T=1/\tau_T$) and $\tau_T^0(=1/k_T^0)$ is intrinsic lifetime of $^3(MAO^+)^*$.

The k_{sq} value was evaluated to be ca. $8\times10^8\ M^{-1}\ s^{-1}$ in water–ethanol mixed solvent. If self-quenching reaction is predominantly due to electron-transfer [14], the semireduced and semioxidized MAO^+ would be anticipated to appear ca. 400 and 750–880 nm, respectively; however, these transient absorption bands may be hidden with the transient bands of $^3(MAO^+)^*$.

The τ_T^0 values evaluated using the band in near-IR region from Eq. (1) (Table 1) were almost same as those evaluated using the band in visible region. The τ_T^0 value in water (ca. 100 μs) [17] is longer than that in ethanol (ca. 1 μs). This tendency is in agreement with the reported one that long triplet lifetimes can be found in polar protic solvents compared to other solvents [34–36]. However, the longest τ_T^0 value was obtained in water:ethanol (1:1, v/v) mixed solvent. In Fig. 5,

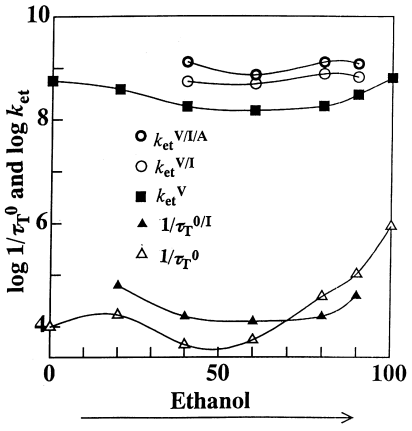

Fig. 5. Plots of $\log 1/\tau_T^0$, $\log 1/\tau_T^{0/I}$, $\log k_{et}^V$, $\log k_{et}^{V/I}$ and $\log k_{et}^{V/I/A}$ vs. ethanol content in ethanol–water mixed solvents.

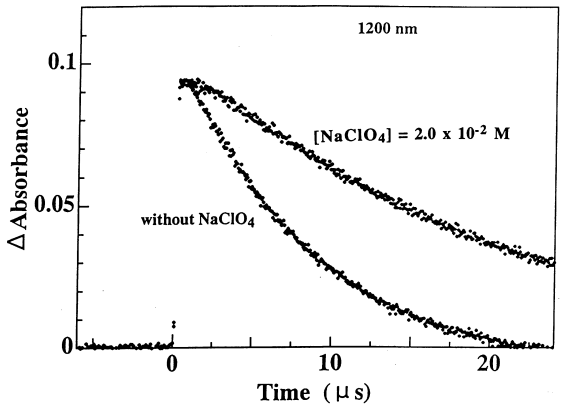

Fig. 6. Decays of $^3(MAO^+)^*$ at 1200 nm in the absence and presence of ionic salt ($NaClO_4$) in ethanol–water (9:1, v/v) mixed solvent.

the $1/\tau_T^0(=k_T^0)$ values are plotted against ethanol content; a minimum is seen at near 40–50% ethanol content.

3.2.2. Ionic salt effect in τ_T^0 values

The decay rate of $^3(MAO^+)^*$ was slowed down on the addition of ionic salt, $NaClO_4$ (Fig. 6), resulting in longer τ_T^0 (Table 1). This may be due to solute–solute (ion–ion) interaction in alcohol-rich mixed solvents [37], which may be decreased by ionic salt effect. However, with increase in water content in the mixed solvents, this effect tends to reverse (Fig. 5), which may be due to some interactions between the salt and $^3(MAO^+)^*$ [38,39].

3.2.3. Quenching of $^3(MAO^+)^*$ with O_2

In the presence of O_2, the decay rates of the absorption band of $^3(MAO^+)^*$ at 1200 nm increased with increasing O_2-concentration (inset in Fig. 4), obeying first-order kinetics. From these decay rates, the second-order rate constants (k_{O_2}) for $^3(MAO^+)^*$-quenching with O_2 was evaluated to be $4.3\times10^9\ M^{-1}\ s^{-1}$, which is very close to the diffusion controlled limit ($k_{diff}=4\times10^9\ M^{-1}\ s^{-1}$ in ethanol–water (4:1, v/v) mixed solvent). For $^3(MAO^+)^*$-quenching with O_2, it would be anticipated that electron transfer and/or energy transfer take place, producing $O_2^{\bullet-}$ and singlet O_2; however, the observation of the absorption and emission of $O_2^{\bullet-}$ and singlet O_2 were obscured by the absorption of MAO^+ and $^3(MAO^+)^*$, respectively.

3.2.4. Reaction of $^3(MAO^+)^*$ with MV^{2+} (oxidative route)

In the presence of MV^{2+}, the transient absorption bands due to $MV^{\bullet+}$ appeared at 380 and 600 nm [13,27–29] with the decay of $^3(MAO^+)^*$ at 1020 and 1200 nm in deaerated ethanol (Fig. 7); inset in Fig. 7 shows the decay and rise time-profiles at 1200 and 380 nm, respectively. Thus, it is proved that electron transfer occurs from $^3(MAO^+)^*$ to MV^{2+}. The transient absorption band of $MV^{\bullet+}$ at 600 nm considerably overlaps with $^3(MAO^+)^*$ at 600 nm. The bands at 750 and 880 nm of $(MAO^+)^{\bullet+}$ [14] decay within 1 μs,

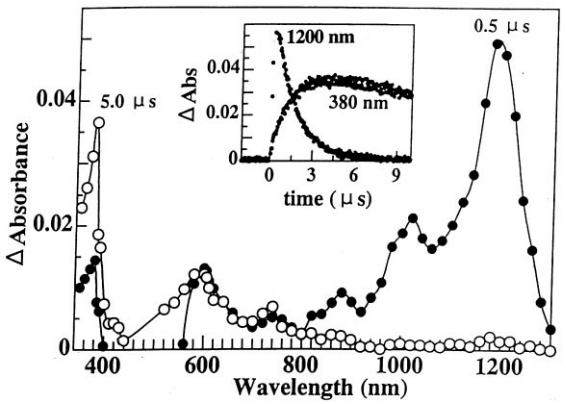

Fig. 7. Transient absorption spectra observed on photolysis of MAO^+ (1.0×10^{-4} M) with 490 nm light in the presence of MV^{2+} (1.0×10^{-3} M) in deaerated ethanol; (●) 0.5 μs and (○) 5.0 μs. Inset: Decay and rise time profiles at 1200 and 380 nm, respectively.

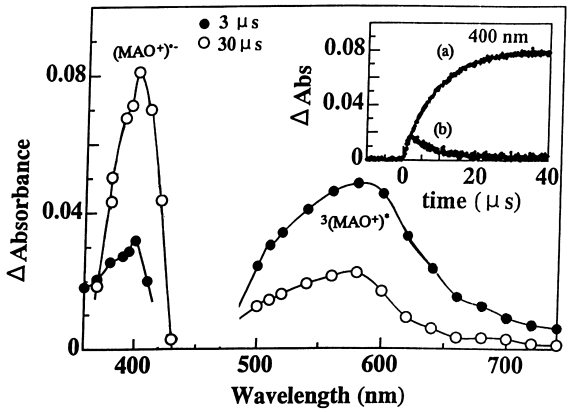

Fig. 8. Transient absorption spectra observed on photolysis of MAO^+ (1.0×10^{-4} M) with 490 nm light in presence of TEOA (1.0×10^{-2} M) in deaerated ethanol–water (4:1, v/v) mixed solvent; (●) 3 μs and (○) 30 μs. Inset: (a) Rise time-profile of $(MAO^+)^{\bullet-}$ in the absence of MV^{2+} and (b) decay time-profile of $(MAO^+)^{\bullet-}$ in the presence of MV^{2+} (2.0×10^{-4} M).

which is probably due to the back electron transfer from $MV^{\bullet+}$ to $(MAO^+)^{\bullet+}$.

From first-order kinetics of the decay of $^3(MAO^+)^*$ in the presence of MV^{2+}, the second-order rate constants (k_{et}^V) for the reaction of $^3(MAO^+)^*$ with MV^{2+} were evaluated as summarized in Table 1. The $\log k_{et}^V$ values in Fig. 5 exhibit a minimum at 60% ethanol content. From Fig. 5, it is also found that the $1/\tau_T^0$ and k_{et}^V values vary similarly. This indicates that the reactivity of $^3(MAO^+)^*$ is mainly affected by solvation of $^3(MAO^+)^*$ itself.

In presence of $NaClO_4$ (the rate constant is abbreviated as $k_{et}^{V/I}$, where suffix I refers to ionic salt), the $k_{et}^{V/I}$ values are slightly higher than the k_{et}^V values (Fig. 5), indicating that $NaClO_4$ promotes dissociation of the ion pairs of $^3(MAO^+)^*$ and MV^{2+} due to the increase in the ionic strength. When TEOA is further added (the rate constant is abbreviated as $k_{et}^{V/I/A}$, where suffix A refers to amine), the $k_{et}^{V/I/A}$ values are also slightly higher than the $k_{et}^{V/I}$ values, indicating that TEOA accelerates the electron-transfer rate from $^3(MAO^+)^*$ to MV^{2+}. Since the electron transfer rate constant (k_{et}^A) from TEOA to $^3(MAO^+)^*$ was evaluated to be $5.5\times10^5\ M^{-1}\ s^{-1}$ in the next section, TEOA may increase the $k_{et}^{V/I/A}$ in indirect ways; on assuming the electron-transfer process is in equilibrium as shown in Scheme 1, TEOA may shift the equilibrium process to the right side.

3.2.5. Reaction of $^3(MAO^+)^*$ with TEOA (reductive route)

In the presence of TEOA, the transient absorption band of $(MAO^+)^{\bullet-}$ appeared at 400 nm [14,17] with the decay of $^3(MAO^+)^*$ at 580 nm in visible region (Fig. 8), indicating that electron transfer occurs from TEOA to $^3(MAO^+)^*$; this process is illustrated in the left side (reductive route) of Scheme 2. The k_{et}^A value was as low as $5.5\times10^5\ M^{-1}\ s^{-1}$. The k_{et}^A values did not change significantly with the solvent composition in water–ethanol mixed solvents.

The inserted time profiles in Fig. 8 show the rise of $(MAO^+)^{\bullet-}$ at 400 nm and its decay-time profile in the presence of MV^{2+}. The slow rise of $(MAO^+)^{\bullet-}$ is in good agreement with the slow decay of $^3(MAO^+)^*$ at 580 and 1200 nm. On addition of MV^{2+} to the solution of MAO^+/TEOA system (inset in Fig. 8), the absorption band of $(MAO^+)^{\bullet-}$ at 400 nm decays obeying first-order kinetics. This implies that $(MAO^+)^{\bullet-}$ donates its excess electron to MV^{2+}, yielding finally $MV^{\bullet+}$ as shown in Scheme 2 (left side). The rate constant for this process (k_{et}^{MV}) was evaluated to be $4.7\times10^8\ M^{-1}\ s^{-1}$. In this case, $MV^{\bullet+}$ remained without decaying, indicating that back electron transfer from $MV^{\bullet+}$ to $TEOA^{\bullet+}$ is inhibited. This may be related to rapid degradation of $TEOA^{\bullet+}$ into the species with low electron accepting ability [6,23]. Thus, it is proved that the persistent $MV^{\bullet+}$ is also formed via the reductive route (Scheme 2).

3.2.6. Decay kinetics of $MV^{\bullet+}$ in the absence of TEOA in oxidative route

Fig. 9A shows the time profiles at 605 nm at long timescale, which was observed when MAO^+ was photoirradiated in the presence MV^{2+} and in the absence of TEOA.

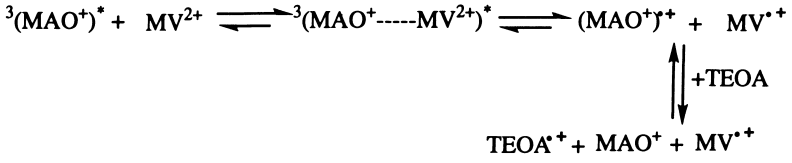

Scheme 1.

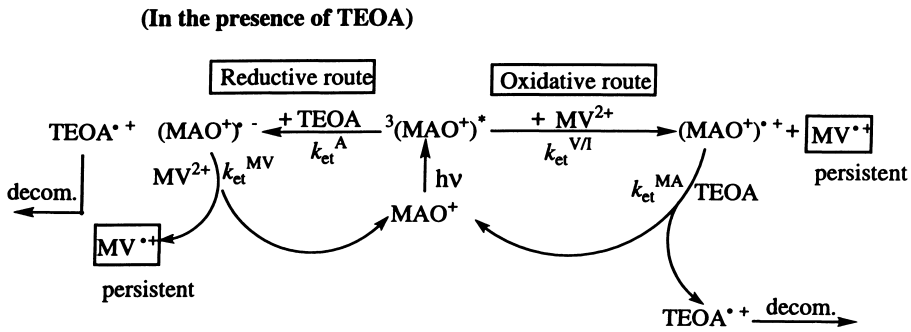

Scheme 2.

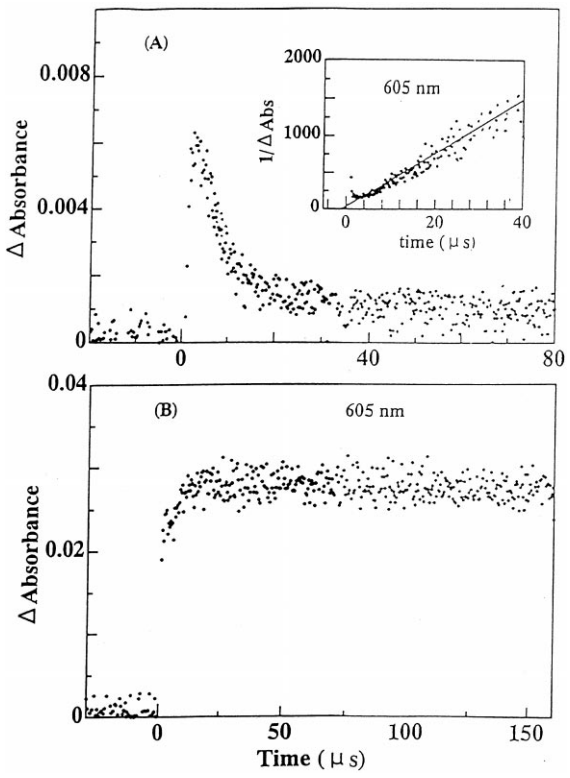

Fig. 9. Time profiles at 605 nm in long time-scale obtained by laser photolysis in ethanol–water (4:1, v/v) mixed solvent. (A) For MAO^+(1.0×10^{-4} M)/MV^{2+}(5.0×10^{-4} M) system (80 μs). Inset: second-order plot. (B) For MAO^+ (1.0×10^{-4} M)/MV^{2+}(5.0×10^{-4} M)/TEOA (1.5×10^{-1} M) system (150 μs).

Compared with the decay of $^3(MAO^+)^*$ in inset of Fig. 7, the observed decay at 605 nm was attributed mainly to the decay of $MV^{\bullet+}$ produced via oxidative route. The decay rate of $MV^{\bullet+}$ obeys second-order kinetics (inset in Fig. 9A), indicating that $MV^{\bullet+}$ reverts back to MV^{2+} by back electron transfer to $(MAO^+)^{\bullet+}$ (k_{bet} in Scheme 3). From the slope ($k_{bet}/\varepsilon_{MV^{\bullet+}}$) of the second-order plot ($1/\Delta$Abs versus time), the k_{bet} value was evaluated to be $3.3\times10^8\,M^{-1}\,s^{-1}$, which is lower than the k_{diff} value by a factor of ca. 10, because of repulsion between cationic species [28]. This finding suggests that the steady-concentration of $MV^{\bullet+}$ during photolysis is not high in the absence of TEOA, because of the back electron transfer from $MV^{\bullet+}$ to $(MAO^+)^{\bullet+}$.

3.2.7. Decay kinetics of $MV^{\bullet+}$ in the presence of TEOA

Fig. 9B shows the time profiles at 605 nm observed by the laser excitation of MAO^+ in the presence of MV^{2+} and excess TEOA. Non-decaying component was observed with the rise within 15 μs. This is attributed to the formation curve of $MV^{\bullet+}$, which is produced by both oxidative and reductive routes. Thus, it is confirmed that the produced $MV^{\bullet+}$ does not decay for a long time, when TEOA is sufficiently present.

The relative contributions for $^3(MAO^+)^*$ decays can be estimated from the ratio of $k_{et}^{V/I/A}[MV^{2+}]_0 : k_{et}^{A}[TEOA]_0$, if the successive electron-transfer rate constants are as large as k_{diff}. When $[MV^{2+}]_0=2.0\times10^{-4}$ M and $[TEOA]_0=1.0\times10^{-2}$ M, the ratio was evaluated to be 1:0.05, which implies that the contribution of electron transfer route from TEOA to $^3(MAO^+)^*$ (reductive route) is only ca. 5%. When $[TEOA]_0$ is increased up to 0.1 M under a constant $[MV^{2+}]_0$, $k_{et}^{V/I/A}[MV^{2+}]_0 : k_{et}^{A}[TEOA]_0 = 2 : 1$, which corresponds to the contribution of the reductive route of 33%. Contribution of oxidative route increases with an increase in MV^{2+} concentration; however, high concentration of MV^{2+} affords extremely high absorbance of $MV^{\bullet+}$, which prohibits the penetration of the excitation light as an internal filter effect in steady-state measurements. Thus, when $[MV^{2+}]_0$ was kept as low as 2.0×10^{-4} M, the number of turn-over $[MV^{\bullet+}]/[MAO^+]_0$ is two; on increase in

(in the absence of TEOA; oxidative route)

$$^3(MAO^+)^* \xrightarrow[k_{et}^{V}]{+MV^{2+}} (MAO^+)^{\bullet+} + MV^{\bullet+} \xrightarrow{k_{bet}} MAO^+ + MV^{2+}$$

Scheme 3.

$[MV^{2+}]_0$, the number of turn-over would be expected to increase, although it takes a more irradiation time to reach maximal $[MV^{\bullet+}]$.

3.2.8. Quantum yields for $MV^{\bullet+}$ formation via oxidative route

The concentrations of $^3(MAO)^*$ and $MV^{\bullet+}$ were evaluated from the initial absorption intensity at 1200 nm and final absorption intensity at 605 nm, respectively, using Eq. (2).

$$\frac{[MV^{\bullet+}]_{max}}{[^3(MAO^+)^*]_{max}} = \frac{(A_V/\varepsilon_V)}{(A_T/\varepsilon_T)} \quad (2)$$

where A and ε refer to maximal absorbance and molar extinction coefficient, respectively; suffix V and T to $MV^{\bullet+}$ and $^3(MAO)^*$, respectively. Upon substitution of the reported $\varepsilon_V$and ε_T values [28,40], $[MV^{\bullet+}]_{max}/[^3(MAO)^*]_{max}$ were evaluated. The plot of $[MV^{\bullet+}]_{max}/[^3(MAO)^*]_{max}$ with $[MV^{2+}]$ reaches a plateau, yielding the quantum yield ($\Phi_{MV^{\bullet+}}$) for electron transfer from $^3(MAO)^*$ to MV^{2+}. The $\Phi_{MV^{\bullet+}}$ values increase with TEOA, reaching maximum at $[TEOA]=1\times10^{-1}$ M in a similar manner to Fig. 3; the values of $\Phi_{MV^{\bullet+}}$ at $[TEOA]=1\times10^{-1}$ M are listed in Table 1.

The $\Phi_{MV^{\bullet+}}$ values vary with changing the composition of ethanol–water mixed solvents with the similar trend to Y_{SF} in Table 1. It is notable that the $\Phi_{MV^{\bullet+}}$ values for $^3(MAO)^*$ are better than the published data for other sensitizer/MV^{2+}/EDTA systems; e.g. $\Phi_{MV^{\bullet+}}=0.55$ for acridine [41] and $\Phi_{MV^{\bullet+}}=0.32$ for $[Ru(bpy)_3]^{2+}$ [3,30].

4. Conclusions

MAO^+ acts as an efficient photosensitizer and electron-mediator in the presence of sacrificial donor to produce persistent $MV^{\bullet+}$ from MV^{2+}. The utilization of the laser flash photolysis method was useful to elucidate the mechanism for both oxidative and reductive routes. Kinetic data affords the relative contributions of two routes to the $MV^{\bullet+}$ formation. Optimum yield was obtained on controlling the TEOA concentration and ionic strength. Solvent constitution of water–ethanol mixed solvents also affects the kinetic behavior.

Acknowledgements

The present work was partly supported by the Grant-in-Aid on General-Research B (No. 11440211) from the Ministry of Education, Science, Sports and Culture of Japan. The authors express their thanks to the referees of this manuscript for their fruitful comments and suggestions.

References

[1] G. Blauer, H. Linschitz, J. Phys. Chem. 66 (1962) 453.
[2] K.D. Asmus, H. Mockel, A. Henglein, J. Phys. Chem. 73 (1969) 2573.
[3] K. Mandal, M.Z. Hoffman, J. Phys. Chem. 88 (1984) 185.
[4] S.H.A. Yoshimura, M.Z. Hoffman, J. Phys. Chem. 98 (1994) 5058.
[5] V.S.F. Chew, R.G. Bolton, R.G. Brown, G. Porter, J. Phys. Chem. 84 (1980) 1909.
[6] M. Georgopolous, M.Z. Hoffman, J. Phys. Chem. 95 (1991) 7717.
[7] J.S. Bellin, G. Oster, J. Am. Chem. Soc. 79 (1957) 2461.
[8] M.S. Chan, J.R. Bolton, Solar Energy 24 (1980) 561.
[9] K. Kalyanasundaram, M. Grtzel, J. Chem. Soc., Chem. Commun. 1979 (1979) 1137.
[10] K. Kalyanasundaram, D. Dung, J. Phys. Chem. 84 (1980) 2551.
[11] M.S. Chan, J.R. Bolton, Photochem. Photobiol. 34 (1981) 537.
[12] J.D. Spikes, R. Straight, Ann. Rev. Phys. Chem. 18 (1967) 409.
[13] M-P. Pileni, M. Grtzel, J. Phys. Chem. 84 (1980) 2402.
[14] A. Kellmann, Photochem. Photobiol. 20 (1974) 103.
[15] C.A. Parker, C.G. Hatchard, T.A. Joyce, Nature 205 (1965) 1282.
[16] S. Solar, W. Solar, N. Getoff, Z. Naturforsch. A. 37 (1982) 1077.
[17] E. Vogelmann, W. Rauscher, H.E.A. Kramer, Photochem. Photobiol. 29 (1979) 771.
[18] A.J. Bard, A. Ledwith, H.J. Shine, Adv. Phys. Org. Chem. 13 (1976) 155.
[19] A.J. Bard, A.B. Bocarsly, F.-R.F. Fan, E.G. Walton, M.S. Wrighton, J. Am. Chem. Soc. 102 (1980) 3671.
[20] A.B. Bocarsly, D.C. Bookbinder, R.N. Dominey, N.S. Lewis, M.S. Wrighton, J. Am. Chem. Soc. 102 (1980) 3683.
[21] C.L. Bird, A.T. Kuhn, Chem. Soc. Rev. 10 (1981) 49.
[22] H. Feilchenfeld, G. Chumanov, T.M. Cotton, J. Phys. Chem. 100 (1996) 4937.
[23] D.R. Prasad, M.Z. Hoffman, Q.G. Mulazzani, M.A. Rodgers, J. Am. Chem. Soc. 108 (1986) 5135.
[24] T. Konishi, Y. Sasaki, M. Fujitsuka, Y. Toba, H. Moriyama, O. Ito, J. Chem. Soc., Perkin Trans. 2 551 (1999).
[25] S.D.-M. Islam, M. Fujitsuka, O. Ito, Phys. Chem. Chem. Phys. 1 (1999) 3737.
[26] L. Costantino, G. Guarino, O. Ortona, V. Vitagliano, J. Chem. Eng. Data. 29 (1982) 63.
[27] A. Harriman, A. Mills, J. Chem. Soc., Faraday Trans. 2 77 (1981) 2111.
[28] T. Watanabe, K. Honda, J. Phys. Chem. 86 (1982) 2617.
[29] Y.-S. Kim, S. McNiven, K. Ikebukuro, I. Karube, Photochem. Photobiol. 66 (1997) 180.
[30] H. Sun, A. Yoshimura, M.Z. Hoffman, J. Phys. Chem. 98 (1994) 5058.
[31] G. Greiner, P. Pasquini, R. Weiland, H. Orthwein, H. Rau, J. Photochem. Photobiol. Chem.: A 51 (1990) 179.
[32] G. Nouchi, J. Chim. Phys. Phys.-Chim. Biol. 66 (1969) 548.
[33] C.V. Kumer, L. Qin, P.K. Das, J. Chem. Soc., Faraday Trans. 2 80 (1984) 783.
[34] J.N. Moorthy, S.L. Monahan, R.B. Sunoj, J. Chandrasekhar, C. Bohne, J. Am. Chem. Soc. 121 (1999) 3093.
[35] J.C. Netto-Ferreira, W.J. Leigh, J.C. Scaiano, J. Am. Chem. Soc. 107 (1985) 2617.
[36] P.J. Wagner, A.E. Kemppainen, H.N. Schott, J. Am. Chem. Soc. 95 (1973) 5604.
[37] H. Fujiwara, T. Kitamura, Y. Wada, S. Yanagida, P.V. Kamat, J. Phys. Chem. A 103 (1999) 4874.
[38] J.C. Scaiano, D. Weldon, C.N. Pliva, L.J. Martinez, J. Phys. Chem. A 102 (1998) 6898.
[39] J.C. Scaiano, J. Am. Chem. Soc. 102 (1980) 7747.
[40] V. Zanker, E. Miethke, Z. Naturforsch. A 12A (1957) 385.
[41] J.R. Darwent, P. Douglas, A. Harriman, G. Portet, M.-C. Richoux, Coord. Chem. Rev. 44 (1982) 83.